atoms

MDPI

Article

Rigorous Negative Ion Binding Energies in Low-Energy Electron Elastic Collisions with Heavy Multi-Electron Atoms and Fullerene Molecules: Validation of Electron Affinities

Alfred Z. Msezane * and Zineb Felfli

Department of Physics and Center for Theoretical Studies of Physical Systems, Clark Atlanta University, Atlanta, GA 30314, USA

* Correspondence: amsezane@cau.edu

Abstract: Dramatically sharp resonances manifesting stable negative ion formation characterize Regge pole-calculated low-energy electron elastic total cross sections (TCSs) of heavy multi-electron systems. The novelty of the Regge pole analysis is in the extraction of rigorous and unambiguous negative ion binding energies (BEs), corresponding to the measured electron affinities (EAs) of the investigated multi-electron systems. The measured EAs have engendered the crucial question: is the EA of multi-electron atoms and fullerene molecules identified with the BE of the attached electron in the ground, metastable or excited state of the formed negative ion during a collision? Inconsistencies in the meaning of the measured EAs are elucidated and new EA values for Bk, Cf, Fm, and Lr are presented.

Keywords: Regge poles; generalized bound states; multi-electron atoms; elastic cross sections; anionic binding energies; electron affinities; electron correlation; core–polarization interaction

Citation: Msezane, A.Z.; Felfli, Z. Rigorous Negative Ion Binding Energies in Low-Energy Electron Elastic Collisions with Heavy Multi-Electron Atoms and Fullerene Molecules: Validation of Electron Affinities. *Atoms* **2023**, *11*, 47. https://doi.org/10.3390/atoms11030047

Academic Editors: Himadri S. Chakraborty and Hari R. Varma

Received: 4 January 2023
Revised: 23 February 2023
Accepted: 27 February 2023
Published: 3 March 2023

1. Introduction

In the electron impact energy range $0.0 \leq E \leq 10.0$ eV, dramatically sharp resonances manifesting stable ground, metastable and excited negative ion formation, shape resonances (SRs), and Ramsauer–Townsend (R-T) minima characterize the Regge pole calculated low-energy electron elastic total cross sections (TCSs) of heavy multi-electron atoms and fullerene molecules [1]. The energy positions of the sharp resonances correspond to the measured electron affinities (EAs) of the considered multi-electron atoms and fullerene molecules. Indeed, the extraction from the TCSs of rigorous and unambiguous negative ion binding energies (BEs), the SRs, and the R-T minima, without any experimental or other theoretical assistance demonstrates the novelty and strength of the Regge pole analysis and its vital importance in the understanding of low-energy electron collisions with complex multi-electron systems through negative ion formation.

The recent theoretical investigation of low-energy electron elastic collisions with heavy multi-electron atoms and fullerene molecules, using Regge pole analysis, also discussed the meaning of the measured EA within two prevailing contexts [1]. The first viewpoint considers the EA to correspond to the electron binding energy when it is attached to the ground state of the formed negative ion during the collision. The second view interprets the EA as corresponding to the BE of the attached electron in an excited state of the formed negative ion. Examples of the first case are the measured EAs of the Au, Pt, and the highly radioactive At atoms [2–7] as well as of the C_{60} and C_{70} fullerene molecules [8–12]. The measured EAs of Nb [13,14], Hf [15], the lanthanide atoms Eu [16,17] and Tm [18], and the actinide atoms Th [19] and U [20,21] as well as the theoretical EAs of Bk, Cf, Fm, and Lr [22–26] represent the second interpretation of the EA. Clearly, whether the measured/calculated EA of heavy multi-electron atoms and fullerene molecules is interpreted as corresponding to the binding energy (BE) of the attached electron in the ground state,

the metastable state, or the excited state of the formed negative ion during the collision, the Regge pole-calculated binding energies provide rigorous and unambiguous energy values.

We demonstrate the second viewpoint of the meaning of the EA by using the Nb atom as an example. The EA of atomic Nb is both interesting and revealing because there are two measured EA values, namely 0.917 eV [13] and 0.894 eV [14] as well as two theoretical EAs 0.82 eV [27] and 0.99 eV [28]. Their interpretation notwithstanding, the agreement among these values is quite good and with the Regge pole-metastable BE value of 0.902 eV. Experimental studies of the lanthanide atoms are challenging due to the difficulty of producing sufficient negative ions for use in photodetachment experiments [16]. Problems concerning the interpretation of what is meant by the measured EAs of the lanthanide atoms have already been discussed [29,30]. For the actinide atoms, the experimental breakthrough using a nanogram of Bk and Cf [31] and the recent first ever EA measurements of the highly radioactive elements At [7], Th [19], and U [20,21] represent significant advances in the measurements of the challenging to handle atoms. In addition, more such measurements in other radioactive atoms can be expected in the near future. Of great concern and puzzle, however, is that the measured [7] and the calculated [32–35] EAs of At correspond to the ground state BE of the formed At^- anion during the collision, while the measured EAs of Th and U are identified with the BEs of the attached electron in the excited states of the formed anions during a collision. Consequently, reliable theoretical predictions and guidance are essential for a fundamental understanding and interpretation of what is actually being measured.

The Regge pole method has been benchmarked on the measured EAs of atomic Au, At, and Eu as well as the C_{60} fullerene molecule through the negative ion BEs extracted from the Regge pole-calculated electron elastic TCSs. For clarity, Table 1 compares the Regge pole-calculated negative ion BEs with measured and calculated EAs of various atoms and fullerene molecules to assess the reliability of the existing measured/calculated EAs. Indeed, from the Eu atom through the end of Table 1, the meaning of the EA is ambiguous and riddled with uncertainty. This is particularly the case with the actinide atoms Bk, Cf, Fm, and Lr, the focus of this paper, and, for these atoms there are no measured EAs available. This explains our focus on them. We determine their ground, metastable, and excited state negative ion BEs from the Regge pole-calculated electron elastic scattering TCSs to understand the existing calculated EAs and assess their reliability. We then present unambiguous and reliable BEs to guide the measurements of their EAs.

Table 1. Negative ion binding energies (BEs) and ground state Ramsauer–Townsend (R-T) minima, all in eV extracted from TCSs of the atoms and the fullerene molecules C_{60} and C_{70}. They are compared with the measured electron affinities (EAs) in eV. GRS, MS-*n*, and EXT-*n* (*n* = 1, 2) refer, respectively, to ground, metastable, and excited states. Experimental EAs, EXPT, and theoretical EAs, theory is also included. The numbers in the square brackets are the references.

System Z	BEs GRS	BEs MS-1	BEs MS-2	EAs EXPT	BEs EXT-1	BEs EXT-2	R-T GRS	BEs/EAs Theory	EAs RCI [23]	EAs GW [24]
Au 79	2.26	0.832	-	2.309 [2] 2.301 [3] 2.306 [4]	0.326	-	2.24	2.50 [27] 2.19 [36] 2.313 [37] 2.263 [38]	-	-
Pt 78	2.16	1.197	-	2.128 [2] 2.125 [5] 2.123 [6]	0.136	-	2.15	2.163 [38]	-	-
At 85	2.42	0.918	0.412	2.416 [7]	0.115	0.292	2.43	2.38 [32] 2.42 [33] 2.412 [34] 2.45 [35]	-	-
C_{60}	2.66	1.86	1.23	2.684 [8] 2.666 [9] 2.689 [10]	0.203	0.378	2.67	2.57 [39] 2.63 [40] 2.663 [41]	-	-

Table 1. *Cont.*

System Z	BEs GRS	BEs MS-1	BEs MS-2	EAs EXPT	BEs EXT-1	BEs EXT-2	R-T GRS	BEs/EAs Theory	EAs RCI [23]	EAs GW [24]
C_{70}	2.70	1.77	1.27	2.676 [9] 2.72 [11] 2.74 [12]	0.230	0.384	2.72	3.35 [42] 2.83 [42]	-	-
Nb 41	2.48	0.902	-	0.917 [13] 0.894 [14]	0.356	-	2.47	0.82 [27] 0.99 [28]	-	-
Eu 63	2.63	1.08	-	0.116 [16] 1.053 [17]	0.116	-	2.62	0.117 [22] 0.116 [43]	-	-
Tm 69	3.36	1.02	-	1.029 [18]	0.016	0.274	3.35	-	-	-
Hf 72	1.68	0.525	-	0.178 [15]	0.017	0.113	1.67	0.114 [44] 0.113 [45]	-	-
Th 90	3.09	1.36	0.905	0.608 [19]	0.149	0.549	3.08	0.599 [19] 0.549 [46]	0.368	1.17
U 92	3.03	1.44	-	0.315 [20] 0.309 [21]	0.220	0.507	3.04	0.175 [47] 0.232 [21]	0.373	0.53
Bk 97	3.55	1.73	0.997	N/A	0.267	0.505	3.56	-	0.031	−0.276 −0.503
Cf 98	3.32	1.70	0.955	N/A	0.272	0.577	3.34	-	0.010 0.018	−0.777 −1.013
Fm 100	3.47	1.79	1.02	N/A	0.268	0.623	3.49	-	-	0.354 0.597
Lr 103	3.88	1.92	1.10	N/A	0.321	0.649	3.90	0.160 [25] 0.310 [25] 0.476 [26]	0.295 0.465	−0.212 −0.313

2. Method of Calculation

Understanding the structure and dynamics of low-energy electron elastic collisions with multi-electron atoms and fullerene molecules, resulting in the formation of stable negative ions, is quite challenging for conventional quantum mechanical methods. Most of the sophisticated methods developed in atomic physics were tasked with reproducing experimental results with high accuracies but did very little to unravel and elucidate the intricate details and the precise description of the nature of the different physical effects important to a particular process; they also lacked the predictive power. Expressing the desired solutions to scattering problems, as a partial wave (PW) series where the summation is over the orbital (or total) angular momentum quantum number, presents a major problem to the conventional quantum mechanical approaches. The PW series is notoriously very slowly convergent, particularly when the wavelength of the incoming particle is much smaller than the range of the scattering potential. The PW expansion may contain hundreds, if not thousands, of terms, with the result that the calculated EAs are generally riddled with uncertainties and therefore difficult to interpret.

However, if the angular momentum is allowed to become complex-valued, this slowly convergent PW series is replaced with a more rapidly converging series. This leads us to the concept of Regge poles. Simply put, Regge poles are generalized bound states, i.e., the solution of the Schrödinger equation where the energy E is real, positive and the angular momentum λ is complex. Here, the rigorous Regge pole method has been used to calculate the electron elastic TCSs. Regge poles, singularities of the S-matrix, rigorously define resonances [48,49] and in the physical sheets of the complex plane, they correspond to bound states [50]. The Regge poles formed during low-energy electron elastic scattering become stable bound states [51]. The near-threshold electron–atom/fullerene collision TCS resulting in negative ion formation as resonances are calculated independently of measurements using the Mulholland formula [52]. This formula converts the infinite discrete sum into a background integral plus the contribution from a few poles to the

process under consideration. Indeed, the method requires no a priori knowledge of the experimental or any other theoretical data as inputs; hence, its predictive nature.

Electron–electron correlations and core–polarization interactions are both crucial for the existence and stability of most negative ions. The former effects are embedded in the Mulholland formula [53,54] for the TCS, while the latter interactions are incorporated through the well-investigated Thomas–Fermi type model potential. Within the CAM, λ description of scattering, Im λ is used to differentiate between the shape resonances (short-lived resonances) and the stable bound states of the negative ions (long-lived resonances) formed as Regge resonances in the electron–atom (molecule) collision. For the latter, the Im λ is several orders of magnitude smaller than that for the former. The Mulholland formula [52] used here is of the form [53,54] (atomic units are used throughout):

$$\begin{array}{l}\sigma_{tot}(\mathrm{E}) \\ = 4\pi k^{-2}\int_0^\infty Re[1-S(\lambda)]\lambda d\lambda \\ -8\pi^2 k^{-2}\sum\limits_n Im\frac{\lambda_n\rho_n}{1+\exp(-2\pi i\lambda_n)} + I(E)\end{array} \quad (1)$$

In Equation (1) $S(\lambda)$ is the S-matrix, $k = \sqrt{2mE}$, with m = 1 being the mass and E the impact energy, ρ_n is the residue of the S-matrix at the nth pole, λ_n and $I(E)$ contains the contributions from the integrals along the imaginary λ-axis (λ is the complex angular momentum); its contribution has been demonstrated to be negligible [55]. In the Regge pole, also known as the complex angular momentum (CAM), method the important and revealing energy-dependent Regge trajectories are also calculated. Their effective use in low-energy electron scattering has been demonstrated in [55,56], for example.

As in [57], we consider the incident electron to interact with the complex heavy system without consideration of the complicated details of the electronic structure of the system itself. Thus, the robust Avdonina–Belov–Felfli potential [58], which embeds the vital core–polarization interaction is used:

$$U(r) = -\frac{Z}{r(1+\alpha Z^{1/3}r)(1+\beta Z^{2/3}r^2)} \quad (2)$$

In Equation (2) Z is the nuclear charge, α and β are variation parameters. For small r, the potential describes Coulomb attraction between an electron and a nucleus, $U(r) \sim -Z/r$, while at large distances it has the appropriate asymptotic behavior, *viz.* $\sim -1/(\alpha\beta r^4)$ and accounts properly for the polarization interaction at low energies. Notably, for an electron, the source of the bound states giving rise to Regge trajectories is the attractive Coulomb well it experiences near the nucleus. The addition of the centrifugal term to the well "squeezes" these states into the continuum [54,59]. For larger CAM, λ the effective potential develops a barrier. Consequently, a bound state crossing the threshold energy E = 0 in this region may become an excited state or a long-lived metastable state. As a result, the highest "bound state" formed during the collision is identified with the highest excited state, here labeled as EXT-1, see Table 1. As E increases from zero, the second excited state may form with the anionic BE labeled, EXT-2. For the metastable states, similar labeling is used as MS-1, MS-2, etc. However, it should be noted here that the metastable states are labeled relative to the anionic ground state. The CAM methods have the advantage that the calculations are based on a rigorous definition of resonances, viz. as singularities of the S-matrix [49,50]. It is noted here that $1/(\mathrm{Im}\ \lambda)$ also determines the angular life of a resonance [50,60].

The strength of this extensively studied potential, Equation (2) [61,62] lies in that it has five turning points and four poles connected by four cuts in the complex plane. The presence of the powers of Z as coefficients of r and r^2 in Equation (2) ensures that spherical and non-spherical atoms and fullerenes are correctly treated. Small and large systems are also appropriately treated. The effective potential $V(r) = U(r) + \lambda(\lambda+1)/2r^2$ is considered here as a continuous function of the variables r and complex λ. The numerical

calculations of the TCSs, limited to the near-threshold energy region, namely below any excitation thresholds to avoid their effects, are obtained by solving the Schrödinger equation as described in [54], see also [63]. The parameters "α" and "β" of the potential in Equation (2) are varied, and with the optimal value of α = 0.2, the β-parameter is further varied carefully until the dramatically sharp resonance appears in the TCS. This is indicative of stable negative ion formation during the collision and the energy position matches with the measured EA of the atom/fullerene molecule; see for example the Au and C_{60} fullerene TCSs in [1]. This has been found to be the case in all the atoms and fullerenes investigated thus far.

Here, we consider the presence of a sufficiently narrow resonance, which allows the collision partners to form a long-lived intermediate complex that rotates as it decays at zero scattering angle to preserve the total angular momentum. If the complex has a large angular life, namely Im λ << 1**,** it will return to forward scattering many times. For the resonance to contribute to the TCS two resonance conditions must be satisfied: (1) Regge trajectory, namely Im λ versus Re λ stays close to the real axis and (2) the real part of the Regge pole is close to an integer.

3. Results

To better understand and appreciate the problem we are discussing here, we first consider the TCSs of the standard atomic Au and C_{60} fullerene molecule, given in Figure 1 of Ref. [1]. Clearly seen from the figure is that in the Au TCSs (left panel of Figure 1) there are three dramatically sharp resonances representing stable negative ion formation in the ground (2.26 eV), metastable (0.832 eV), and excited (0.326 eV) states of the formed negative ions during the collision. In the C_{60} fullerene TCSs (right panel of Figure 1) there are five dramatically sharp resonances, corresponding to the ground state BE (2.66 eV), two metastable BEs (1.86 eV and 1.23 eV), and two excited state BEs (0.378 eV and 0.203 eV). In both cases, the measured EAs of the Au atom and the C_{60} fullerene molecule correspond to the anionic BEs of the attached electron in the ground states of the formed anions during the collision, see also Table 1. Importantly, the delineation of the dramatically sharp resonances in the TCSs of both Au and C_{60} ensures the correct interpretation of what is being measured. It is noted here that both the Au and C_{60} TCSs also abound in SRs and R-T minima. Similarly, for Pt, At, and C_{70} the measured EAs correspond to the BEs of the electron when it is attached to the ground states of the formed negative ions (see Table 1 here). Indeed, this excellent agreement gives great credence to the Regge pole analysis to produce rigorous and unambiguous BEs without any assistance from either experiment or any other theory, as well as to our interpretation of the EAs of these complex systems, viz. as corresponding to the ground state BEs of the formed negative ions during the collisions.

Recall that the primary objective of this paper is to subject the measured and/or calculated EAs of the investigated atoms and fullerene molecules in this paper to the Regge pole-calculated ground, metastable, and excited state negative ion BEs of the formed anions during the collisions for unambiguous interpretation of the EAs. Here, the presented Figures 1 and 2 of the TCSs demonstrate the clear delineation of the dramatically sharp resonances leading to the unambiguous determination of the ground, metastable, and excited state BEs of the formed negative ions during the collisions. Table 1 summarizes the BEs of the various atoms and fullerenes, extracted from the TCSs of the atoms of interest here and compares them with the measured/calculated EAs.

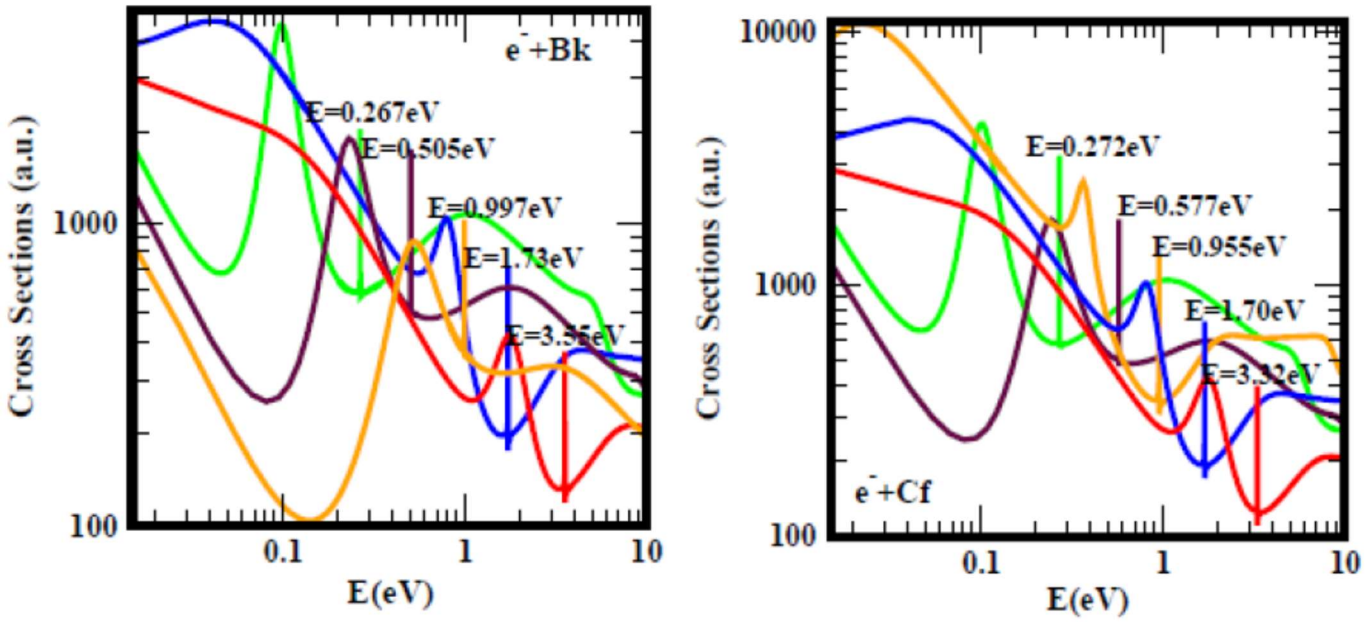

Figure 1. Total cross sections (a.u.) for electron elastic scattering from atomic Bk (**left panel**) and Cf (**right panel**) are contrasted. For both Bk and Cf the red, blue, and orange curves represent TCSs for the ground and the two metastable states, respectively, while the brown and the green curves correspond to excited state TCSs. The dramatically sharp resonances in the TCSs of both figures correspond to the Bk^- and Cf^- negative ions formed during the collisions. Importantly, the flip over of the near-threshold R-T minimum from the Bk TCSs to an SR very close to threshold in the Cf TCSs occurs here.

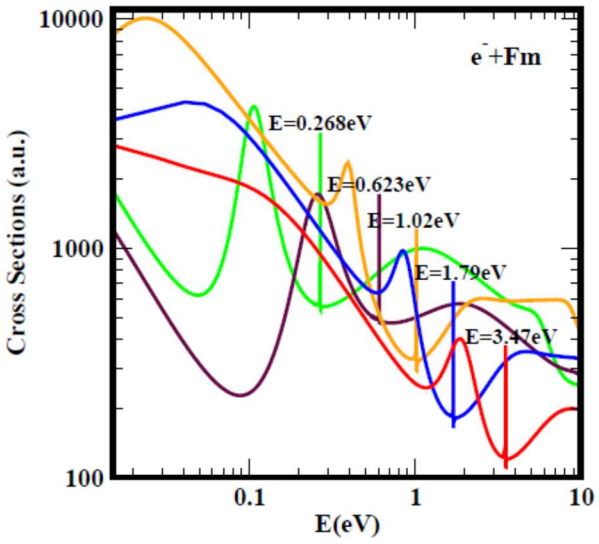

Figure 2. *Cont.*

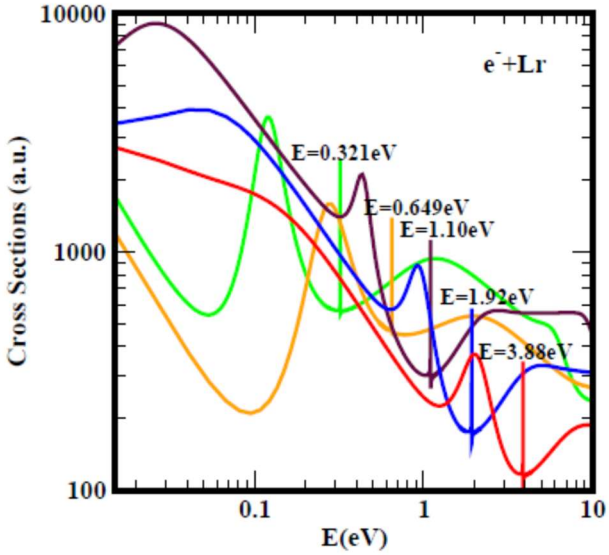

Figure 2. Total cross sections (a.u.) for the actinide atoms Fm (**top panel**) and Lr (**bottom panel**). In both panels the red curves represent the ground states. In Fm the blue and the orange curves and in Lr the blue and the brown curves are the metastable TCSs while the brown and the green curves in Fm and the orange and the green curves in Lr represent the excited state TCSs. The energy positions of the dramatically sharp lines correspond to electron BEs of the formed negative ions during collisions. The orange curve in the TCSs for Fm and the brown curve in those for Lr correspond to the polarization-induced TCSs with the deep R-T minima flipped over to SRs close to threshold (see also Figure 1 above).

The ambiguous and confusing EAs of the actinide atoms in particular, from Th through Lr have necessitated the careful evaluation/assessment of the measured and/or calculated EAs in order to determine their meaning. As seen from Table 1, it is particularly difficult to make sense of the existing theoretical EAs of the Bk, Cf, Fm, and Lr actinide atoms. Therefore, here, we demonstrate the importance and effective use of the Regge pole-calculated BEs by comparing them with the EAs of the listed atoms in Table 1, particularly the four actinide atoms above. To this end, we have grouped our discussions for convenience as follows: 3.1 Bk and Cf atoms: the interest in them is that a recent experiment probed their structure and dynamics using a nanogram matter; 3.2 Fm and Lr atoms: being at the end of the actinide series, have several calculated EAs available to compare with; 3.3 Relativistic effects in electron affinity calculations.

As seen from Table 1, for atomic Nb the measured and the calculated EAs agree very well, and with the Regge pole metastable BE of 0.902 eV, the ground and the excited state BEs are 2.48 eV and 0.356 eV, respectively. The latest measured EA (0.116 eV) [16] of Eu is in outstanding agreement with the Regge pole BE of 0.116 eV and with the MCDF-RCI EA of 0.117 eV [22]. Yet, the Regge pole value corresponds to an excited state BE of Eu. Notably, the previously measured EA of 1.053 eV [17] and the Regge pole-metastable BE of 1.08 eV for Eu agree excellently. Furthermore, the 1.029 eV measured EA of Tm [18] and the Regge pole BE of 1.02 eV also agree excellently. From Table 1, since the measured EA of Hf [15] is close to the RCI EA [44] and the Regge pole BE of an excited state [45], the measured EA of Hf is identified with the BE of an excited state of Hf contrary to the cases of the Au, Pt, and At atoms as well as of the fullerenes. Consequently, from the measured EAs of Nb, Eu, Tm, and Hf the simple question follows: Does the measured EA of these atoms correspond to the BE of the attached electron in an excited state of the formed anion during the collision?

For Th, the measured and the calculated EAs [19] 0.608 eV and 0.599 eV, respectively, are close to the Regge pole SR at 0.61 eV and the second excited state BE of 0.549 eV [46]. The measured EAs of U 0.315 eV [20] and 0.309 eV [21] with the calculated EA of 0.232 eV [21] are close to each other and to the Regge pole BE of the first excited state of the formed U^-

anion, the MCDF-RCI EA value of 0.175 eV [47] and the 0.373 eV GW EA [24]. However, the Regge pole BE value of the second excited state, 0.507 eV agrees very well with the EA calculated by the GW method 0.53 eV [24]. Here, we are confronted with the inconsistency in the identification of what is actually being measured.

3.1. Bk and Cf Atoms

The selection of the Bk and Cf TCSs presented in Figure 1 is motivated by the rigorous probing of their electronic structure and dynamics through the Regge pole-calculated R-T minima and SRs, revealing their sensitivity [1]. Importantly, the flipping over of the deep R-T minimum in the Bk TCSs to an SR very close to the threshold occurs in the metastable TCS of the Cf atom: see the orange curves in Figure 1. The results of probing their electronic structure and dynamics by the experiment [31] as well as our validation of the observation [1] should help in the measurements of the EAs of Bk and Cf. In Table 1 we have presented our Regge pole anionic BEs for both Bk and Cf and compared them with the existing theoretical EAs: these are riddled with uncertainty and lack reliability. The same conclusion applies to the data of the remaining atoms.

3.2. Fm and Lr Atoms

There are no measured EAs for these atoms; therefore, reliable predictions of their EAs are essential. As the size of the actinide atoms approaches that of the Lr atom, their electronic structure becomes less complicated and the theoretical EAs are expected to become less uncertain. Figure 2 compares the TCSs of the Fm and Lr atoms, selected because of the availability of several theoretical EAs to compare with the Regge pole-calculated BEs. The TCSs of both atoms are characterized by well-delineated dramatically sharp resonances, representing in each atom a ground, two metastable, and two excited state BEs, see also Table 1. Worth remarking here is that in both the TCSs of Fm and Lr the sharp resonances of interest here, although well-delineated from each other, appear close to SRs; this can create problems in the identification of the BEs as seen in Figure 2.

For Fm, it is seen that the Regge pole BEs of the highest excited anionic state (0.268 eV) and the second excited anionic state (0.623 eV) agree rather well with the existing theoretical EA values of 0.354 eV [24] and 0.597 eV [24], respectively. Importantly, the reason why these theoretical EAs differ from each other is that they correspond to different anionic states: this demonstrates the need for rigorous values of the EAs for Fm and the other actinide atoms in general to guide measurements and/or calculations. We note here that the Fm TCSs still exhibit fullerene behavior [64], while in Lr the fullerene behavior has completely disappeared (see green curves in both figures of Figure 2). This almost atomic behavior of the Lr TCSs makes the Lr much easier to handle theoretically as evidenced below.

The importance of the Lr TCSs is two-fold: 1) The electronic structure of Lr is relatively simple and various sophisticated theoretical methods have calculated its EA, see Table 1. On comparing the TCSs of the Fm and Lr atoms, we see that the characteristic SRs appear very near threshold in both TCSs. Since the Lr atom is the last of the actinide series, sophisticated theoretical methods can be expected to obtain better values for the EA of Lr. Indeed, as seen in Figure 2, the TCSs are characterized by well-delineated ground (3.88 eV), two metastable (1.92 eV; 1.10 eV), and two excited (0.321 eV; 0.649 eV) state anionic BEs. Once the determination has been made regarding what anionic state BE was measured/calculated, then by comparison with the above values, an unambiguous EA determination can be obtained as was performed with the Au, Pt, At, and the fullerene molecules in Table 1. However, several calculated EAs are available; we will attempt to make sense of their meaning. Firstly, the 0.310 eV [25], 0.295 eV [23], and the Abs (−0.313 eV) [24] EAs can safely be identified with the Regge pole's highest excited state BE (0.321 eV) and secondly, the EA values of 0.465 eV [23] and 0.476 eV [26] could probably be identified with the Regge pole BE of the second excited state 0.649 eV; they could also correspond to the nearby shape resonance at 0.451 eV, see Figure 2.

Indeed, from Table 1 it is clear that for the actinide atoms, the various sophisticated theoretical methods calculate only the BEs of the formed negative ions in excited states and equate them with the EAs. There is nothing wrong with this viewpoint, except that a rigorous definition of the EA is required for consistency throughout the tabulated atoms and fullerenes in Table 1. This would then mean using the BEs in column BEs, EXT-1 for the corresponding EAs of all the atoms and fullerene molecules in Table 1. Unfortunately, this would contradict the established meaning of the EAs as found for the Au, Pt, and At atoms as well as for the C_{60} and C_{70} fullerenes. It is further noted here that for the carefully measured and calculated EA of At, various sophisticated theoretical EAs [32–35] agree excellently among themselves and with the measured EA as well as with the Regge pole ground state anionic BE and not with the metastable or the excited state anionic BEs. Unfortunately, it is a formidable task for most theoretical methods to calculate the BEs of metastable states, let alone the ground state BEs of the tabulated systems in Table 1.

These results are also important in guiding sophisticated theoretical methods on the importance of polarization interaction. This has been demonstrated unequivocally in the TCSs calculation of the Bk and Cf atoms, particularly in the At atom. When the β-parameter of Equation (2) was 0.042 we obtained the ground state anionic BE value of 2.51 eV [65], which was close to the then known theoretical EA value of 2.80 eV [66]. However, careful refinement of the β-parameter to 0.04195 yielded the ground state BE value of 2.42 eV, in excellent agreement with the measured EA of 2.416 eV [7] and the theoretical values [32–35]. Here, it is noted that the small Im (λ) decreased from 1.07×10^{-5} to 8.9×10^{-6}, indicative that the BE value of 2.42 eV corresponds to the longest-lived resonance as expected (see the importance of the use of Im (λ) in the Regge pole analysis in Ref. [55]). Indeed, a scientific will is needed to respond critically to the question: why are the EAs of Au, Pt, and At as well as those of the C_{60} and C_{70} fullerene molecules identified with the BEs of the formed negative ions in the ground states while for Th and U as well as for the other actinide atoms the EAs correspond to the Regge pole-calculated BEs of excited states? Notably, the Regge pole BEs are available to guide the EA measurements, regardless of their interpretation, namely whether they are viewed as corresponding to the BEs of electron attachment in the ground or excited states.

3.3. Relativistic Effects in Electron Affinity Calculations

The EA provides a stringent test of theoretical calculations when the calculated EAs are compared with those from reliable measurements. Unfortunately, low-energy electron interactions with heavy multi-electron atoms and fullerene molecules are characterized generally by the presence of many intricate and diverse electron configurations. These lead to computational complexity that, for a long time, made it virtually impossible for sophisticated theoretical methods to reliably predict the electron binding energies of the formed negative ions during collisions. Thus, the electron affinities calculated using many structure-based theoretical methods tend to be riddled with uncertainties making them difficult to interpret, particularly for the actinide atoms, see Table 1.

One of the most important and revealing investigations of the importance of Regge trajectories in low-energy electron collisions using the ABF potential, Equation (2), was carried out by Thylwe [56]. For the Xe atom, Regge trajectories calculated using the Dirac relativistic and non-relativistic methods were contrasted near the threshold and found to yield essentially the same Re λ(E) when the Im λ(E) was still very small, see Figure 2 of [56]. This implies the insignificant difference between the relativistic and non-relativistic calculations at low-energy electron scattering, which is the condition of our calculations here.

Most of the sophisticated theoretical calculations of the EAs include relativistic effects at various levels of approximations, see for example their comparisons in the calculation of the EA of At in Ref. [34]. Since many of these methods are tailored to reproduce the measurements very well, it is difficult to determine what essential physics is incorporated in the calculation of the EAs. For instance, Wesendrup et al. [36] carried out large-scale

fully relativistic Dirac–Hartree–Fock and MP2 as well as nonrelativistic pseudo-potential calculations and obtained the EAs of Au as 2.19 eV and 1.17 eV, respectively. In addition, Cole and Perdew [27] employed relativistic and nonrelativistic calculations obtaining the EA of atomic Au as 2.5 eV and 1.5 eV, respectively. These EAs should be compared with the nonrelativistic Regge pole-calculated BE value of 2.263 eV [1,38] and the measured EAs presented in Table 1. Accordingly, it can be safely concluded that in the energy regime, $0.0 \leq E \leq 10.0$ eV the essential physics embedded in the Regge pole method such as electron–electron correlations and core–polarization interaction is adequate for the reliable prediction of the EAs of multi-electron atoms and fullerene molecules. Importantly, an impressive agreement with the measured EAs of Au [2–4] has been obtained by the relativistic coupled cluster calculations with variational quantum electrodynamics [37]; it also supports the Regge pole-calculated BE value.

The calculation of the EA of Nb ($Z = 41$) in [27] used a gradient-corrected exchange-correlation functional and a Nb scalar relativistic core, obtaining an EA value of 0.82 eV, which compares very well with the Regge pole metastable BE value of 0.902 eV and the measured EA values of 0.917 eV [13] and 0.894 eV [14]. These results for Nb further demonstrate the great need to ascertain precisely the state from whence the photodetachment process originates. The Eu atom, with a relatively high Z of 63, but a small, measured EA of 0.116 eV [16], provides a stringent test of the nonrelativistic Regge pole method when its BE value of 0.116 eV [43,55] is contrasted with the MCDF-RCI calculated EA value of 0.117 eV [22]. The theoretical results were calculated around 2009 while the experimental EA was measured in 2015. For the highly radioactive At atom the recently measured EA [7], which employed the coupled cluster method, agreed excellently with the Regge pole BE and the EAs from various sophisticated theoretical calculations, including the multiconfiguration Dirac–Hartree–Fock values [32–35], see Table 1 for comparisons. Furthermore, in [32,34] extensive comparisons among various sophisticated theoretical EAs have been carried out as well.

4. Summary and Conclusions

For the multi-electron atoms and the fullerene molecules considered in this paper, we presented rigorous and unambiguous ground, metastable, and excited state negative ion BEs extracted from the Regge pole-calculated TCSs. We then compared our BEs with the existing measured and/or calculated EAs as shown in Table 1. We found that for the Au, Pt, and At atoms as well as the C_{60} and C_{70} fullerene molecules, our ground state anionic BEs matched excellently with the measured EAs, implying that the measured EAs of these systems correspond to the BEs of the electron when it is attached in the ground states of the formed negative ions during the collision. However, for the lanthanide atom Eu, our excited state BE is in outstanding agreement with both the recently measured and the MCDF-RCI calculated EA values. For both the Eu and Tm atoms, good agreement between the Regge pole-metastable BEs and the previously measured EAs [17,18] has been realized. Overall, our excited state BEs are closer to the measured and/or calculated EAs of the Hf and the actinide atoms. This implies that for these atoms the measured and/or calculated EAs correspond to the BEs of the electron when it is attached in the excited states of the formed negative ions, contrary to the cases of the Au, Pt, and At atoms as well as the C_{60} and C_{70} fullerene molecules.

In conclusion, for the actinide atoms Bk, Cf, Fm, and Lr, we presented the Regge pole-calculated electron elastic TCSs demonstrating their richness in very sharp resonances representing negative ion formation in the ground, metastable, and excited states. From the positions of the dramatically sharp resonances in the TCSs, we extracted the BEs of the formed negative ions during the collisions. These BEs have been compared with the existing theoretical EAs to understand and make sense of these data since they are generally riddled with uncertainties, particularly those of the Bk and Cf atoms. There are no measured EAs for these atoms to compare with our BEs. It is hoped that the results of this paper will inspire and assist both measurements and theory in the determination of the long-overdue

unambiguous and reliable EAs of the actinide atoms. It is noted that the TCSs of these actinide atoms also abound in SRs and R-T minima, making it challenging to extract the EAs. It is hoped that the actinide atoms will be subjected to similar investigations as in [32,34] for unambiguous and reliable EAs. The great strength of the Regge pole analysis is in its use of Im λ(E) to differentiate among the ground, metastable, and excited negative ionic states, with the ground state having the smallest Im λ(E), indicative of the longest-lived negative ionic state.

Author Contributions: Z.F. and A.Z.M. are responsible for the conceptualization, methodology, investigation, formal analysis, and writing of the original draft, as well as rewriting and editing. A.Z.M. is also responsible for securing the funding for the research. All authors have read and agreed to the published version of the manuscript.

Funding: Research was supported by the U.S. DOE, Division of Chemical Sciences, Geosciences and Biosciences, Office of Basic Energy Sciences, Office of Energy Research, Grant: DE-FG02-97ER14743. The computing facilities of the National Energy Research Scientific Computing Center, also funded by the U.S. DOE are greatly appreciated.

Institutional Review Board Statement: Not applicable.

Informed Consent Statement: Not applicable.

Data Availability Statement: Not applicable.

Conflicts of Interest: The authors declare no conflict of interest or state.

References

1. Msezane, A.Z.; Felfli, Z. Recent Progress in Low-Energy Electron Elastic-Collisions with Multi-Electron Atoms and Fullerene Molecules. *Atoms* **2022**, *10*, 79. [CrossRef]
2. Hotop, H.; Lineberger, W.C. Dye-laser photodetachment studies of Au^-, Pt^-, PtN^-, and Ag^-. *J. Chem. Phys.* **2003**, *58*, 2379–2387. [CrossRef]
3. Andersen, T.; Haugen, H.K.; Hotop, H. Binding Energies in Atomic Negative Ions: III. *J. Phys. Chem. Ref. Data* **1999**, *28*, 1511–1533. [CrossRef]
4. Zheng, W.; Li, X.; Eustis, S.; Grubisic, A.; Thomas, O.; De Clercq, H.; Bowen, K. Anion photoelectron spectroscopy of $Au^-(H_2O)_{1,2}$, $Au_2^-(D_2O)_{1-4}$, and $AuOH^-$. *Chem. Phys. Lett.* **2007**, *444*, 232–236. [CrossRef]
5. Gibson, D.; Davies, B.J.; Larson, D.J. The electron affinity of platinum. *J. Chem. Phys.* **1993**, *98*, 5104–5105. [CrossRef]
6. Bilodeau, R.C.; Scheer, M.; Haugen, H.K.; Brooks, R.L. Near-threshold laser spectroscopy of iridium and platinum negative ions: Electron affinities and the threshold law. *Phys. Rev. A* **1999**, *61*, 012505. [CrossRef]
7. Leimbach, D.; Karls, J.; Guo, Y.; Ahmed, R.; Ballof, J.; Bengtsson, L.; Pamies, F.B.; Borschevsky, A.; Chrysalidis, K.; Eliav, E.; et al. The electron affinity of astatine. *Nat. Commun.* **2020**, *11*, 3824. [CrossRef]
8. Huang, D.-L.; Dau, P.D.; Liu, H.T.; Wang, L.-S. High-resolution photoelectron imaging of cold C_{60}^- anions and accurate determination of the electron affinity of C_{60}. *J. Chem. Phys.* **2014**, *140*, 224315. [CrossRef]
9. Brink, C.; Andersen, L.H.; Hvelplund, P.; Mathur, D.; Voldstad, J.D. Laser photodetachment of C_{60}^- and C_{70}^- ions cooled in a storage ring. *Chem. Phys. Lett.* **1995**, *233*, 52–56. [CrossRef]
10. Wang, X.-B.; Ding, C.F.; Wang, L.-S. High resolution photoelectron spectroscopy of C_{60}^-. *J. Chem. Phys.* **1999**, *110*, 8217–8220. [CrossRef]
11. Boltalina, O.V.; Sidorov, L.N.; Sukhanova, E.V.; Skokan, E.V. Electron affinities of higher fullerenes. *Rapid Commun. Mass Spectrom.* **1993**, *7*, 1009–1011. [CrossRef]
12. Palpant, B.; Otake, A.; Hayakawa, F.; Negishi, Y.; Lee, G.H.; Nakajima, A.; Kaya, K. Photoelectron spectroscopy of sodium-coated C_{60} and C_{70} cluster anions. *Phys. Rev. B.* **1999**, *60*, 4509. [CrossRef]
13. Luo, Z.; Chen, X.; Li, J.; Ning, C. Precision measurement of the electron affinity of niobium. *Phys. Rev. A* **2016**, *93*, 020501. [CrossRef]
14. Feigerle, C.S.; Corderman, R.R.; Bobashev, S.V.; Lineberger, W.C. Binding energies and structure of transition metal negative ions. *J. Chem. Phys.* **1981**, *74*, 1580–1598. [CrossRef]
15. Tang, R.; Chen, X.; Fu, X.; Wang, H.; Ning, C. Electron affinity of the hafnium atom. *Phys. Rev. A* **2018**, *98*, 020501. [CrossRef]
16. Cheng, S.-B.; Castleman, A.W. Direct experimental observation of weakly-bound character of the attached electron in europium anion. *Sci. Rep.* **2015**, *5*, 12414. [CrossRef]
17. Davis, V.T.; Thompson, J.S. An experimental investigation of the atomic europium anion. *J. Phys. B* **2004**, *37*, 1961. [CrossRef]
18. Davis, V.T.; Thompson, J.S. Measurement of the electron affinity of thulium. *Phys. Rev. A* **2001**, *65*, 010501. [CrossRef]
19. Tang, R.; Si, R.; Fei, Z.; Fu, X.; Lu, Y.; Brage, T.; Liu, H.; Chen, C.; Ning, C. Candidate for Laser Cooling of a Negative Ion: High-Resolution Photoelectron Imaging of Th^-. *Phys. Rev. Lett.* **2019**, *123*, 203002. [CrossRef]

20. Tang, R.; Lu, Y.; Liu, H.; Ning, C. Electron affinity of uranium and bound states of opposite parity in its anion. *Phys. Rev. A* **2021**, *103*, L050801. [CrossRef]
21. Ciborowski, S.M.; Liu, G.; Blankenhorn, M.; Harris, R.M.; Marshall, M.A.; Zhu, Z.; Bowen, K.H.; Peterson, K.A. The electron affinity of the uranium atom. *J. Chem. Phys.* **2021**, *154*, 224307. [CrossRef]
22. O'Malley, S.M.; Beck, D.R. Valence calculations of lanthanide anion binding energies: 6p attachments to 4fn6s2 thresholds. *Phys. Rev. A* **2008**, *78*, 012510. [CrossRef]
23. O'Malley, S.M.; Beck, D.R. Valence calculations of actinide anion binding energies: All bound 7p and 7s attachments. *Phys. Rev. A* **2009**, *80*, 032514. [CrossRef]
24. Guo, Y.; Whitehead, M.A. Electron affinities of alkaline-earth and actinide elements calculated with the local-spin-density-functional theory. *Phys. Rev. A* **1989**, *40*, 28. [CrossRef] [PubMed]
25. Eliav, E.; Kaldor, U.; Ishikawa, Y. Transition energies of ytterbium, lutetium, and lawrencium by the relativistic coupled-cluster method. *Phys. Rev. A* **1995**, *52*, 291. [CrossRef]
26. Borschevsky, A.; Eliav, E.; Vilkas, M.J.; Ishikawa, Y.; Kaldor, U. Transition energies of atomic lawrencium. *Eur. Phys. J. D* **2007**, *45*, 115–119. [CrossRef]
27. Cole, L.A.; Perdew, J.P. Calculated electron affinities of the elements. *Phys. Rev. A* **1982**, *25*, 1265. [CrossRef]
28. Calaminici, P.; Mejia-Olvera, R.J. Structures, Frequencies, and Energy Properties of Small Neutral, Cationic, and Anionic Niobium Clusters. *Phys. Chem. C* **2011**, *115*, 11891–11897. [CrossRef]
29. Felfli, Z.; Msezane, A.Z.J. Conundrum in Measured Electron Affinities of Complex Heavy Atoms. *J. At. Mol. Condens. Matter Nano Phys.* **2018**, *5*, 73–80. [CrossRef]
30. Felfli, Z.; Msezane, A.Z. Low-Energy Electron Elastic Total Cross Sections for Ho, Er, Tm, Yb, Lu, and Hf Atoms. *Atoms* **2020**, *8*, 17. [CrossRef]
31. Müller, A.; Deblonde, G.J.P.; Ercius, P.; Zeltmann, S.E.; Abergel, R.J.; Minor, A.M. Probing electronic structure in berkelium and californium via an electron microscopy nanosampling approach. *Nat. Commun.* **2021**, *12*, 948. [CrossRef]
32. Si, R.; Froese Fischer, C. Electron affinities of At and its homologous elements Cl, Br, I. *Phys. Rev. A* **2018**, *98*, 052504. [CrossRef]
33. Li, J.; Zhao, Z.; Andersson, M.; Zhang, X.; Chen, C. Theoretical study for the electron affinities of negative ions with the MCDHF method. *J. Phys. B* **2012**, *45*, 165004. [CrossRef]
34. Borschevsky, A.; Pašteka, L.F.; Pershina, V.; Eliav, E.; Kaldor, U. Ionization potentials and electron affinities of the superheavy elements 115–117 and their sixth-row homologues Bi, Po, and At. *Phys. Rev. A* **2015**, *91*, 020501. [CrossRef]
35. Sergentu, D.; David, G.; Montavon, G.; Maurice, R.; Galland, N. Scrutinizing "Invisible" astatine: A challenge for modern density functionals. *J. Comput. Chem.* **2016**, *37*, 1345–1354. [CrossRef]
36. Wesendrup, R.; Laerdahl, J.K.; Schwerdtfeger, P. Relativistic effects in gold chemistry. VI. Coupled cluster calculations for the isoelectronic series AuPt−, Au2, and AuHg+. *J. Chem. Phys.* **1999**, *110*, 9457–9462. [CrossRef]
37. Pašteka, L.F.; Eliav, E.; Borschevsky, A.; Kaldor, U.; Schwerdtfeger, P. Relativistic Coupled Cluster Calculations with Variational Quantum Electrodynamics Resolve the Discrepancy between Experiment and Theory Concerning the Electron Affinity and Ionization Potential of Gold. *Phys. Rev. Lett.* **2017**, *118*, 023002. [CrossRef] [PubMed]
38. Felfli, Z.; Msezane, A.Z.; Sokolovski, D. Near-threshold resonances in electron elastic scattering cross sections for Au and Pt atoms: Identification of electron affinities. *J. Phys. B* **2008**, *41*, 105201. [CrossRef]
39. Nagase, S.; Kabayashi, K. Theoretical study of the lanthanide fullerene CeC82. Comparison with ScC82, YC82 and LaC82. *Chem. Phys. Lett.* **1999**, *228*, 106–110. [CrossRef]
40. Zakrzewski, V.G.; Dolgounitcheva, O.; Ortiz, J.V. Electron propagator calculations on the ground and excited states of C60−. *J. Phys. Chem. A* **2014**, *118*, 7424–7429. [CrossRef]
41. Felfli, Z.; Msezane, A.Z. Simple method for determining fullerene negative ion formation. *Eur. Phys. J. D* **2018**, *72*, 78. [CrossRef]
42. Tiago, M.L.; Kent, P.R.C.; Hood, R.Q.; Reboredo, F. A Neutral and charged excitations in carbon fullerenes from first-principles many-body theories. *J. Chem. Phys.* **2008**, *129*, 084311. [CrossRef] [PubMed]
43. Felfli, Z.; Msezane, A.Z.; Sokolovski, D. Complex angular momentum analysis of low-energy electron elastic scattering from lanthanide atoms. *Phys. Rev. A* **2010**, *81*, 042707. [CrossRef]
44. Pan, L.; Beck, D.R. Calculations of Hf− has only one bound state, electron affinity and photodetachment partial cross sections. *J. Phys. B At. Mol. Opt. Phys.* **2010**, *43*, 025002. [CrossRef]
45. Felfli, Z.; Msezane, A.Z.; Sokolovski, D. Strong resonances in low-energy electron elastic total and differential cross sections for Hf and Lu atoms. *Phys. Rev. A* **2008**, *78*, 030703. [CrossRef]
46. Felfli, Z.; Msezane, A.Z. Negative Ion Formation in Low-Energy Electron Collisions with the Actinide Atoms Th, Pa, U, Np and Pu. *Appl. Phys. Res.* **2019**, *11*, 52. [CrossRef]
47. Dinov, K.D.; Beck, D.R. Electron affinities and hyperfine structure for U− and U I obtained from relativistic configuration-interaction calculations. *Phys. Rev. A* **1995**, *52*, 2632. [CrossRef]
48. Frautschi, S.C. *Regge Poles and S-Matrix Theory*; Benjamin: New York, NY, USA, 1963; Chapter X.
49. D'Alfaro, V.; Regge, T.E. *Potential Scattering*; North-Holland: Amsterdam, The Netherlands, 1965.
50. Omnes, R.; Froissart, M. *Mandelstam Theory and Regge Poles: An Introduction for Experimentalists*; Benjamin: New York, NY, USA, 1963; Chapter 2.
51. Hiscox, A.; Brown, B.M.; Marletta, M. On the low energy behavior of Regge poles. *J. Math. Phys.* **2010**, *51*, 102104. [CrossRef]

52. Mulholland, H.P. An asymptotic expansion for Σ(2n+1)exp (Àσ(n+1/2)2). *Proc. Camb. Philos. Soc.* **1928**, *24*, 280–289. [CrossRef]
53. Macek, J.H.; Krstic, P.S.; Ovchinnikov, S.Y. Regge Oscillations in Integral Cross Sections for Proton Impact on Atomic Hydrogen. *Phys. Rev. Lett.* **2004**, *93*, 183203. [CrossRef] [PubMed]
54. Sokolovski, D.; Felfli, Z.; Ovchinnikov, S.Y.; Macek, J.H.; Msezane, A.Z. Regge oscillations in electron-atom elastic cross sections. *Phys. Rev. A* **2007**, *76*, 012705. [CrossRef]
55. Felfli, Z.; Msezane, A.Z.; Sokolovski, D. Resonances in low-energy electron elastic cross sections for lanthanide atoms. *Phys. Rev. A* **2009**, *79*, 012714. [CrossRef]
56. Thylwe, K.W. On relativistic shifts of negative-ion resonances. *Eur. Phys. J. D* **2012**, *66*, 7. [CrossRef]
57. Dolmatov, V.K.; Amusia, M.Y.; Chernysheva, L.V. Electron elastic scattering off A@C60: The role of atomic polarization under confinement. *Phys. Rev. A* **2017**, *95*, 012709. [CrossRef]
58. Felfli, Z.; Belov, S.; Avdonina, N.B.; Marletta, M.; Msezane, A.Z.; Naboko, S.N. Regge poles trajectories for nonsingular potentials: The Thomas-Fermi Potentials. In Proceedings of the Third International Workshop on Contemporary Problems in Mathematical Physics, Cotonou, Republic of Benin, 1–7 November 2003; Govaerts, J., Hounkonnou, M.N., Msezane, A.Z., Eds.; World Scientific: Singapore, 2004; pp. 217–232.
59. Sokolovski, D.; Msezane, A.Z.; Felfli, Z.; Ovchinnikov, S.Y.; Macek, J.H. What can one do with Regge poles? *Nucl. Instrum. Methods Phys. Res. Sect. B* **2007**, *261*, 133–137. [CrossRef]
60. Connor, J.N.L. New theoretical methods for molecular collisions: The complex angular-momentum approach. *J. Chem. Soc. Faraday Trans.* **1990**, *86*, 1627–1640. [CrossRef]
61. Belov, S.; Thylwe, K.-E.; Marletta, M.; Msezane, A.Z.; Naboko, S.N. On Regge pole trajectories for a rational function approximation of Thomas–Fermi potentials. *J. Phys. A* **2010**, *43*, 365301. [CrossRef]
62. Belov, S.; Avdonina, N.B.; Marletta, M.; Msezane, A.Z.; Naboko, S.N. Semiclassical approach to Regge poles trajectories calculations for nonsingular potentials: Thomas–Fermi type. *J. Phys. A* **2004**, *37*, 6943. [CrossRef]
63. Burke, P.G.; Tate, C. A program for calculating regge trajectories in potential scattering. *Comput. Phys. Commun.* **1969**, *1*, 97–105. [CrossRef]
64. Msezane, A.Z.; Felfli, Z. New insights in low-energy electron-fullerene interactions. *Chem. Phys.* **2018**, *503*, 50–55. [CrossRef]
65. Felfli, Z.; Msezane, A.Z.; Sokolovski, D. Slow electron elastic scattering cross sections for In, Tl, Ga and At atoms. *J. Phys. B* **2012**, *45*, 045201. [CrossRef]
66. Zollweg, R.J. Electron Affinities of the Heavy Elements. *J. Chem. Phys.* **1969**, *50*, 4251–4261. [CrossRef]